OPEN

Septal and Anterior Reverse Mismatch of Myocardial Perfusion and Metabolism in Patients With Coronary Artery Disease and Left Bundle Branch Block

Jian-Guang Wang, MD, Wei Fang, MD, Min-Fu Yang, MD, Yue-Qin Tian, MD, Xiao-Li Zhang, MD, Rui Shen, MD, Xiao-Xin Sun, MD, Feng Guo, MD, Dao-Yu Wang, MD, and Zuo-Xiang He, MD

Abstract: The effects of left bundle branch block (LBBB) on left ventricular myocardial metabolism have not been well investigated. This study evaluated these effects in patients with coronary artery disease (CAD).

Sixty-five CAD patients with complete LBBB (mean age, 61.8 ± 9.7 years) and 65 without LBBB (mean age, 59.9 ± 8.4 years) underwent single photon emission computed tomography, positron emission tomography, and contrast coronary angiography. The relationship between myocardial perfusion and metabolism and reverse mismatch score, and that between QRS length and reverse mismatch score and wall motion score were evaluated.

The incidence of left ventricular septum and anterior wall reverse mismatching between the 2 groups was significantly different ($P < 0.001$ and $P = 0.002$, respectively). The incidences of normal myocardial perfusion and metabolism in the left ventricular lateral and inferior walls were also significantly different between the 2 group ($P < 0.001$ and $P < 0.001$, respectively). The incidence of septal reverse mismatching in patients with mild-to-moderate perfusion was significantly higher among those with LBBB than among those without LBBB ($P < 0.001$). In CAD patients with LBBB, septal reverse mismatching was significantly more common among those with mild-to-moderate perfusion than among those with severe perfusion defects ($P = 0.002$). The correlation between the septal reverse mismatch score and QRS length was significant ($P = 0.026$).

In patients with CAD and LBBB, septal and anterior reverse mismatching of myocardial perfusion and metabolism was frequently present; the septal reverse mismatch score negatively correlated with the QRS interval.

(*Medicine* 94(20):e772)

Key Words:: CAD, LBBB, myocardial metabolism, myocardial perfusion, reverse mismatch.

Abbreviations: ^{18}F-FDG = ^{18}F-fluorodeoxyglucose, ^{99m}Tc-MIBI = ^{99m}Tc-methoxyisobutyl isonitrile, CAD = Coronary Artery Disease, CT = computed tomography, DCM = dilated cardiomyopathy, IMP = intramyocardial pressure, LBBB = Left Bundle Branch Block, LVEF = Left ventricular ejection fraction, PET = positron emission tomography, SPECT = single-photon emission computed tomography.

INTRODUCTION

The prevalence of coronary artery disease (CAD) is significantly higher in patients with left bundle branch block (LBBB) than in those without LBBB.[1] LBBB induces inhomogeneous activation and deformation of the ventricles, leading to inefficient contraction[2] and causing delayed activation of the left ventricle.[3] Spontaneous LBBB is associated with increased cardiovascular and overall mortalities.[4–6]

Assessment of myocardial perfusion by single-photon emission computed tomography (SPECT) is commonly performed in patients with LBBB to detect CAD.[7] However, most previous studies evaluating the characteristics of myocardial perfusion imaging in LBBB patients[8–11] have focused on patients with LBBB and dilated cardiomyopathy (DCM)[3,12–15] or with LBBB and ischemic cardiomyopathy.[15,16] Rest myocardial perfusion SPECT with technetium compounds is useful for localising healed myocardial infarction in patients with LBBB, and exercise (+dipyridamole) SPECT has a high positive predictive value and specificity for the diagnosis of coronary stenosis in these patients.[17] ^{18}F-fluorodeoxyglucose (^{18}F-FDG) myocardial metabolic imaging showed septal uptake reduced in relation to septal ^{99m}Tc-methoxyisobutyl isonitrile (^{99m}Tc-MIBI) uptake, and is defined ''reversed mismatch.''[8–10,18] Most of these studies included patients with DCM;[2,3,12,13] few have reported results from patients with ischemic cardiomyopathy[16] or CAD.[8–10]

This study evaluated the characteristics of myocardial perfusion and metabolism in patients with angiographically significant CAD and LBBB. Furthermore, the correlations of the reverse mismatch scores with the QRS durations and with the echocardiographic wall motion scores were assessed.

MATERIALS AND METHODS

Study Patients

Sixty-five consecutive patients with complete LBBB and suspected or known CAD underwent ^{99m}Tc-MIBI SPECT, ^{18}F-FDG positron emission tomography (PET), and, between July 2009 and July 2013, to evaluate their myocardial viability at Fu Wai Hospital (Beijing, China), and underwent coronary angiography were included in this study. A control group was

Editor: Partha Sinha.
Received: December 22, 2014; revised: March 16, 2015; accepted: March 23, 2015.
From the Department of Nuclear Medicine, State Key Laboratory of Cardiovascular Disease, Fu Wai Hospital, National Center for Cardiovascular Disease, Chinese Academy of Medical Sciences and Peking Union Medical College, (J-GW, WF, Y-QT, X-LZ, RS, X-XS, FG, D-YW, Z-XH); Department of Nuclear Medicine, Beijing Chao-Yang Hospital, Capital Medical University, Beijing, People's Republic of China (M-FY).
Correspondence: Zuo-Xiang He, MD, Distinguished Professor and Chairman, Department of Nuclear Medicine, Fu Wai Hospital, 167, Bei Li Shi Lu, Beijing 100037, People's Republic of China (e-mail: zuoxianghe@hotmail.com).
The authors have no conflicts of interest to disclose.

ISSN: 0025-7974
DOI: 10.1097/MD.0000000000000772

also included that comprised consecutive patients undergoing ^{99m}Tc-MIBI SPECT, ^{18}F-FDG PET, and coronary angiography between June 2011 and April 2013. The clinical and imaging data were retrospectively reviewed and analyzed. Patients were excluded if they had myocarditis, valvular heart disease, hypertrophic cardiomyopathy, alcoholic cardiomyopathy, or diastolic heart failure. All patients provided signed informed consent, and the study was approved by the institutional review board.

Electrocardiography

LBBB was defined as a QRS duration ≥120 ms; presence of large, flat or notched R wave in the V5 lead; large, deep S wave showing QS or rS wave in V1 and V2 leads (II, III, aVF and V1 is similar);secondary ST-T wave changes, where the QRS complex up leads(eg I,aVL,V5,etc.) ST segment depression, T waves inversion, main wave in the QRS complex down leads (eg II, aVR,V1, etc) ST-segment elevation, T wave upright.QRS duration is measured from the beginning of the Q wave to the end of the S wave. A normal range is from 40 to 100 milliseconds (1 small box to 2.5 small boxes).

Coronary Angiography

Standard selective coronary angiography was performed within 1 month of the SPECT and PET examinations. Stenosis classification: 1, without stenosis; 2, mild stenosis (<30%); 3, moderate stenosis (30%–50%); 4, severe stenosis (50%–90%); 5, subtotal occlusion (>90%); 6, total occlusion, no blood. Stenosis with ≥50% diameter narrowing were considered significant.

Echocardiography

Resting 2-dimensional echocardiography was performed within 2 weeks of the PET study using a 2.5-MHz, multifrequency probe in harmonic imaging mode. Patients took a left lateral decubitus position and were asked to breathe calmly. Wall motion of the left ventricle was visually evaluated using digital cine loop analysis or tissue Doppler imaging in the apical 4- and 3-chamber views, parasternal short axis views of left ventricle. After obtaining the images, the left ventricle is divided 17 sections according to the American Heart Association recommended method. Left ventricular ejection fraction (LVEF) was measured by the Simpson rule.

^{99m}Tc-MIBI SPECT

Myocardial perfusion ^{99m}Tc-MIBI SPECT acquisition was performed using a dual-head gamma camera (e.cam; Siemens Healthcare, Erlangen Germany); 90–120 min after injection of 740 MBq of ^{99m}Tc-MIBI, at rest, perfusion images were acquired with 64 views (25 s per view) using a zoom factor of 1.23. The cardiac cycle was divided into 8 equal intervals. Images were reconstructed using standard, filtered back-projection with a Butterworth filter (cut-off frequency, 0.4 cycles/cm; order, 5.0) and displayed as short-axis and horizontal and vertical long-axis slices.

^{18}F-FDG PET

Myocardial ^{18}F-FDG PET/computed tomography (CT) and ^{99m}Tc-MIBI SPECT imaging were performed within 2 days of each other. After an overnight fast of at least 12 h, an oral glucose solution (25–50 g, based on patient serum glucose levels) was administered. Insulin was intravenously administered if the blood glucose level was >9.0 mmol/L, 45 min after administration of the oral glucose solution, with close monitoring of the blood glucose levels.[19] When the blood glucose level was appropriate, ^{18}F-FDG (3 MBq/kg) was intravenously administered.[19] Images were acquired 1–2 h after tracer injection using a Biograph 64 PET/CT scanner (Siemens Healthcare) equipped with high-performance lutetium oxyorthosilicate PET crystals and a 64-slice CT. After a scout CT acquisition (120 kV, 10 mA) was performed to ensure proper patient positioning, a CT transmission scan (140 kV, 35 mA) was performed for attenuation correction and anatomical localization. Images were reconstructed using attenuation-weighted ordered subset expectation maximization iterative reconstruction (8 subsets, 4 iterations).

Image Analysis

Based on the standard 17-segment model, the perfusion and metabolism images were visually evaluated by 2 nuclear physicians, blinded to the clinical data. Perfusion imaging segments were scored using a 5-point scoring system (0, normal; 1, mild defect; 2, moderate defect; 3, severe defect; and 4, absent tracer); PET images were scored using the same scoring system. The following terminology was also employed to describe the myocardial perfusion and metabolism: Normal, normal myocardial perfusion and metabolism; Match, concordant reduction of myocardial perfusion and metabolism; Mismatch, reduced myocardial perfusion with preserved metabolism; and Reverse Mismatch, reduced metabolism in comparison with myocardial perfusion. Echocardiographic wall motion was scored using a 4-point scale (1, normal; 2, hypokinetic; 3, akinetic; and 4, dyskinetic).

TABLE 1. Patient Characteristics

Characteristics	CAD With LBBB	CAD Without LBBB	*P*
Men (total)	58 (65)	56 (65)	0.595
Age (years)	61.8 ± 9.7	59.9 ± 8.4	0.217
Smoking, n	29	36	0.221
Hypertension, n	40	33	0.218
Hyperlipidemia, n	44	35	0.107
Diabetes mellitus, n	27	25	0.721
Old myocardial infarction, n	49	50	0.838
Revascularization, n	16	15	0.838
Coronary angiography, n			
Normal	2		
LAD* stenosis	10	1	
LCx stenosis	2		
RCA stenosis	4		
Ramus	1		
LAD/LCx	5	2	
LAD/RCA	8	12	
LCx/RCA		1	
LAD/LCx/RCA	33	49	
QRS, ms	149.9 ± 21.6	94.8 ± 12.2	<0.001
LVEF, %	35.5 ± 8.5	44.4 ± 11.2	<0.001

CAD = coronary artery disease, LAD = left anterior descending artery, LBBB = left bundle branch block, LCx = left circumflex artery, LVEF = left ventricular ejection fraction, NS = not statistically significant, QRS = ??, RCA = right coronary artery.

Statistical Analysis

All variables were reported as means ± SD or frequencies when appropriate. Student's *t*-test was used to compare mean differences in continuous variables between the 2 patient groups. Likewise, a chi-squared test was used to compare categorical variables between the 2 groups. Correlations between 2 variables were obtained using Spearman's test. Data analyses were performed using SPSS, version 13.0 (IBM, Armonk, NY). A 2-tailed P-value < 0.05 was considered statistically significant.

RESULTS

Patient Characteristics

A total of 65 CAD patients with and 65 patients without LBBB underwent ^{99m}Tc-MIBI SPECT, ^{18}F-FDG PET, and coronary angiography. As shown in Table 1, the numbers of men and the average ages of the patients in the groups were not significantly different. CAD patients, with or without LBBB, had similar frequencies of smoking, hypertension, hyperlipidemia, diabetes mellitus, old myocardial infarctions, and histories of revascularization. LVEF was lower in the patients with LBBB than in those without LBBB. The QRS duration in LBBB patients was also higher than in patients without LBBB.

Characteristics of Myocardial Perfusion and Metabolism Imaging

Results of the regional perfusion-metabolism relationship for all patients are shown in Table 2; only 5 patients showed normal septal myocardial perfusion and metabolism on imaging. The incidences of septal and anterior reverse mismatch were significantly different between patients with and without LBBB (56.9% vs 9.3%, $\chi^2 = 33.4$, $P < 0.001$; 18.5% vs 1.5%, $P = 0.002$, respectively) (Table 2). Normal myocardial perfusion and metabolism in the lateral and inferior walls was significantly different between the 2 groups (84.6% vs 21.5%, $\chi^2 = 51.9$, $P < 0.001$; 30.8% vs 4.6%, $P < 0.001$, respectively) (Table 2). Similarly, reverse mismatching in the apex was also significantly different between the 2 groups ($P < 0.001$) (Table 2). A typical case of myocardial perfusion and metabolism reverse mismatch is illustrated in Figure 1.

Septal mismatching and septal reverse mismatching between the 2 groups, in patients with mild to moderate myocardial perfusion was significantly different (30.0% vs 67.6%, $\chi^2 = 7.386$, $P = 0.007$; 60.0% vs 2.7%, $\chi^2 = 24.8$, $P < 0.001$, respectively) (Table 3). Nevertheless, the lateral, anterior, inferior, and apex wall matched, mismatched, and reverse mismatched incidences were not significantly different (Table 3). Moreover, the incidences of matched, mismatched, and reverse mismatched myocardial perfusion and metabolism were not significantly different among the patients with severe perfusion defects (Table 4).

In the CAD patients with LBBB, the incidences of septal match, septal reverse mismatch, and anterior match of myocardial perfusion and metabolism between patients with mild to moderate and severe perfusion defects were significantly different (10.0% vs 62.5%, $\chi^2 = 8.789$, $P = 0.003$; 60.0% vs 6.25%, $\chi^2 = 9.554$, $P = 0.002$; 29.4% vs 58.8%, $\chi^2 = 4.113$, $P = 0.043$, respectively) (Table 5). In these same patients, the septal mismatch; lateral wall match and mismatch; anterior wall mismatch and reverse mismatch; inferior wall match and mismatch; and apical match, mismatch, and reverse mismatch were no significantly different between the patients with mild to moderate perfusion defects and those with severe defects (Table 5).

TABLE 2. Wall Characteristics of Coronary Artery Disease Patients With and Without (control) Left Bundle Branch Block (LBBB)

	LBBB	Control	χ^2	*P*	Odds Ratio
Septum, n					
Normal	5 (7.7)			0.058	
Match	12 (18.5)	24 (36.9)	5.5	0.019	0.387
Mismatch	11 (16.9)	35 (53.8)	19.4	<0.001	0.175
Reverse Mismatch	37 (56.9)	6 (9.3)	33.4	<0.001	13.0
Lateral, n					
Normal	55 (84.6)	14 (21.5)	51.9	<0.001	20.0
Match	4 (6.2)	16 (24.6)	7.2	0.007	0.201
Mismatch	6 (9.2)	33 (50.8)	26.7	<0.001	0.099
Reverse Mismatch		2 (3.1)		0.496	
Anterior, n					
Normal	8 (12.3)	2 (3.1)	2.700	0.100	
Match	20 (30.7)	32 (49.2)	4.615	0.032	0.458
Mismatch	25 (38.5)	30 (46.2)	0.788	0.375	
Reverse Mismatch	12(18.5)	1 (1.5)		0.002	14.5
Inferior, n					
Normal	20 (30.8)	3 (4.6)	13.5	<0.001	9.2
Match	14 (21.5)	16 (24.6)	0.011	0.916	
Mismatch	30 (46.2)	44 (67.7)	6.1	0.013	0.409
Reverse Mismatch	1 (1.5)	2 (3.1)	0.000	>0.99	
Apex, n					
Normal	9 (13.9)			0.003	0.862
Match	21 (32.3)	33 (50.8)	4.6	0.033	0.463
Mismatch	21 (32.3)	32 (49.2)	3.9	0.050	0.492
Reverse Mismatch	14 (21.5)			<0.001	0.785

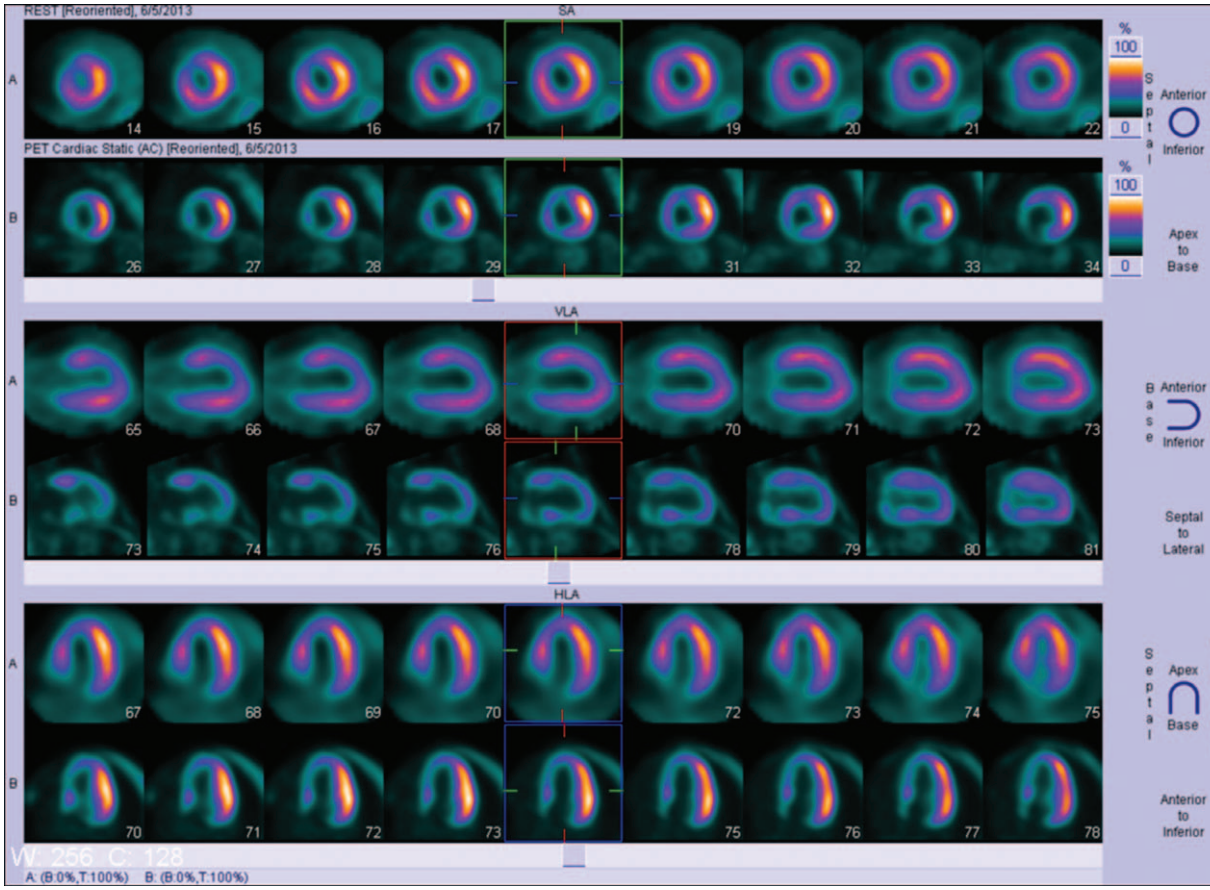

FIGURE 1. A 72-year-old man with symptoms of angina, but no history of myocardial infarction. His risk factors included hypertension, hyperlipidemia, and diabetes mellitus. Resting electrocardiography showed left bundle branch block, and coronary angiography shows total ostial occlusion of the left anterior descending artery.

CORRELATION BETWEEN REVERSE MISMATCH SCORE AND QRS LENGTH AND BETWEEN REVERSE MISMATCH SCORE AND WALL MOTION SCORE

The correlations between the reverse mismatch scores and QRS lengths are shown in Table 6 and Figure 2. The QRS length negatively correlated with the septal reverse mismatch score ($r = -0.276$, $P = 0.026$), whereas associations were not observed with the anterior, apex, lateral, or inferior reverse mismatch scores (Table 6). Similarly, a statistically significant correlation was not observed between the wall motion scores and reverse mismatch scores (Table 6).

DISCUSSION

This study involved a reasonably large cohort of CAD patients with and without LBBB who underwent myocardial SPECT and ^{18}F-FDG PET imaging to evaluate septal myocardial perfusion and metabolism. We demonstrated that the majority of CAD with LBBB patients have septal and anterior reverse perfusion and metabolism mismatching, as determined using SPECT and PET imaging. Additionally, septal reverse mismatching of myocardial perfusion and metabolism was present in CAD patients with LBBB and mild-to-moderate myocardial perfusion defects. Finally, there was a significant negative correlation between the QRS length and the reverse septal mismatch score in CAD patients with LBBB.

Previous Studies in Patients with DCM and LBBB

Masci et al. reported a study involving DCM patients with (11) and without (7) LBBB; 29 (60%), 14 (29%), and 5 (10%) of the 48 investigated segments had flow metabolism reverse mismatching in the septum, adjacent regions, and lateral regions, respectively.[2] In another group of 15 patients with DCM and LBBB, ^{18}F-FDG uptake was highest in the lateral wall and the lowest in the septum, with intermediate values for the anterior and posterior walls.[3] Another group of 8 DCM patients with LBBB was reported to have severe septal defects, as indicated by ^{18}F-FDG uptake and septal flow metabolism reverse mismatching.[13]

Previous Studies in Patients With CAD and LBBB

Zanco et al. reported that 29 patients with complete LBBB, but no significant stenosis during coronary angiography, showed reduced septal ^{18}F-FDG uptake compared to ^{13}N-NH_3 uptake. The reverse mismatch involved 18%, 35%, and 47% of the anterior walls, inferior walls, and both walls, respectively; none of the patients had a lateral region reverse mismatch.[18] In another group of 6 patients with CAD, the septal FDG/MIBI ratio was significantly lower in patients with LBBB (0.62 ± 0.12) than in those without LBBB (1.24 ± 0.24, $P < 0.001$) and did not exceed 0.8 in patients with LBBB.[8] Further, a study involving 53 patients with LV dysfunction and ischemic cardiomyopathy showed that among 34 patients with LBBB, 23 (68%) demonstrated septal reverse mismatching and

TABLE 3. Wall Characteristics in Patients With Mild to Moderate Perfusion

	LBBB	Control	χ^2	*P*	Odds Ratio
Septum, n					
Match	2 (10.0)	11 (29.7)	1.725	0.189	
Mismatch	6 (30.0)	25 (67.6)	7.386	0.007	0.206
Reverse mismatch	12 (60.0)	1 (2.7)	24.8	<0.001	55.5
Lateral, n					
Match	3 (37.5)	16 (35.6)	0.000	>0.99	
Mismatch	5 (62.5)	27 (60.0)	0.000	>0.99	
Reverse mismatch		2 (4.4)		>0.99	
Anterior, n					
Match	10 (29.4)	14 (43.75)	1.465	0.226	
Mismatch	19 (55.9)	17 (53.125)	0.051	0.822	
Reverse mismatch	5 (14.7)	1 (3.125)	2.012	0.156	
Inferior, n					
Match	5 (33.3)	7 (25.0)	0.337	0.561	
Mismatch	10 (66.7)	21 (75.0)	0.337	0.561	
Reverse mismatch					
Apex, n					
Match	2 (25.0)	8 (44.4)		0.420	
Mismatch	4 (50.0)	10 (55.6)		>0.99	
Reverse Mismatch	2 (25.0)			0.086	

LBBB = left bundle branch block.

11 (32%) did not.[16] In our study, the overall incidence of myocardial flow metabolism reverse mismatching was 56.9% in the septum, 18.5% in the anterior segment, and 21.5% in the apex, similar to the findings of the previous studies.

Patients with complete LBBB demonstrate severely reduced ^{18}F-FDG uptake, but preserved septal uptake of the long-chain fatty acid analog ^{18}F-fluoro-6-thia-heptadecanoate and ^{11}C-acetate. Altehoefer et al. reported 1 patient with 3-vessel disease, a history of previous anterior myocardial infarction, and LBBB who showed severely reduced ^{18}F-FDG uptake but preserved septal uptake of ^{18}F-fluoro-6-thia-heptadecanoic acid in the interventricular septum and septal portions of the anterior and posterior walls.[9] Zanco et al. described a patient with insulin-dependent diabetes who had significant left anterior descending artery stenosis, thrombolyzed myocardial infarction, and complete LBBB, despite severe damage on ^{18}F-FDG.[10]

TABLE 4. Wall Characteristics in Patients With Severe Perfusion Defects

	LBBB	Control	χ^2	*P*
Septum, n				
Match	10 (62.5)	13 (54.2)	0.273	0.601
Mismatch	5 (31.25)	9 (37.5)	0.165	0.685
Reverse mismatch	1 (6.25)	2 (8.3)	0.000	>0.99
Lateral, n				
Match	1 (50.0)			0.286
Mismatch	1 (50.0)	5 (100.0)		0.286
Anterior, n				
Match	10 (58.8)	18 (58.1)	0.003	0.959
Mismatch	6 (35.3)	13 (41.9)	0.202	0.653
Reverse mismatch	1 (5.9)			0.354
Inferior, n				
Match	9 (31.0)	9 (28.1)	0.062	0.804
Mismatch	20 (69.0)	23 (71.9)	0.062	0.804
Apex, n				
Match	19 (50.0)	25 (53.2)	0.086	0.770
Mismatch	17 (44.7)	22 (46.8)	0.036	0.849
Reverse mismatch	2 (5.3)			0.197

LBBB = left bundle branch block.

TABLE 5. Comparison of Wall Characteristics Among Patients With Coronary Artery Disease and Left Branch Bundle Block (LBBB), Depending on Perfusion Defect Severity

	Mild to Moderate	Severe to Defect	χ^2	*P*	Odds Ratio
Septum, n					
Match	2 (10.0)	10 (62.5)	8.789	0.003	0.067
Mismatch	6 (30.0)	5 (31.25)	0.000	>0.99	
Reverse mismatch	12 (60.0)	1 (6.25)	9.554	0.002	24.000
Lateral, n					
Match	3 (37.5)	1 (50.0)	0.000	>0.99	
Mismatch	5 (62.5)	1 (50.0)	0.000	>0.99	
Anterior, n					
Match	10 (29.4)	10 (58.8)	4.113	0.043	0.292
Mismatch	19 (55.9)	6 (35.3)	1.922	0.166	
Reverse mismatch	5 (14.7)	1 (5.9)	0.213	0.645	
Inferior, n					
Match	5 (33.3)	9 (31.0)	0.024	0.877	
Mismatch	10 (66.7)	20 (69.0)	0.024	0.877	
Apex, n					
Match	2 (25.0)	19 (50.0)	0.810	0.368	
Mismatch	4 (50.0)	17 (44.7)	0.000	>0.99	
Reverse mismatch	2 (25.0)	2 (5.3)	1.233	0.267	

The Correlation of the QRS Interval and Myocardial Perfusion and Reverse Mismatch Score

Few studies have found correlations among the QRS interval, ^{18}F-FDG uptake, and ^{99m}Tc-MIBI myocardial perfusion.[20] Castro et al. reported that in patients with LBBB and nonischemic heart failure, global heterogeneity in ^{18}F-FDG uptake was highly correlated with QRS length ($r = 0.62$, $P = 0.002$); no correlation was found between ^{18}F-FDG uptake standard deviation and LVEF ($r = 0.12$; $P = 0.57$).[20] In our study of patients with CAD, the septum reverse mismatch scores were significantly correlated with the QRS interval ($r = -0.276$, $P = 0.026$).

Correlation Between Wall Motion Scores of Echocardiography and Reverse Mismatch Score

A previous study demonstrated paradoxical septal wall motion in 33% of patients with LBBB, and wall thickening abnormalities were observed in 49% of those patients. However, no differences in wall motion or wall thickening abnormalities were observed between LBBB patients with and without CAD.[7] Regional findings in LBBB patients reflect delayed conduction and asynchronous contraction of the septal and lateral walls, as demonstrated by echocardiography; without a correlation between the reverse mismatch and wall motion scores.[12]

TABLE 6. Correlation of the Reverse Mismatch Score With the QRS Interval and Wall Motion Scores in Patients With Coronary Artery Disease and Left Branch Bundle Block

	r	*P*
QRS length and reverse mismatch score		
Septum	−0.276	0.026*
Anterior	−0.154	0.221
Apex	−0.079	0.532
Lateral	−0.186	0.138
Inferior	−0.086	0.495
Reverse mismatch score and wall motion score		
Septum	0.083	0.509
Anterior	0.004	0.973
Apex	0.176	0.160
Lateral	−0.051	0.687
Inferior	0.093	0.463

QRS = ??.

The Mechanism of Myocardial Perfusion and Metabolism

The mechanism of myocardial perfusion and metabolism mismatching remains unclear, but several hypotheses exist regarding the mechanism of abnormal septal perfusion and metabolism. Ho et al. showed that LBBB may be caused by functional ischemia due to asynchronous septal contraction.[21]

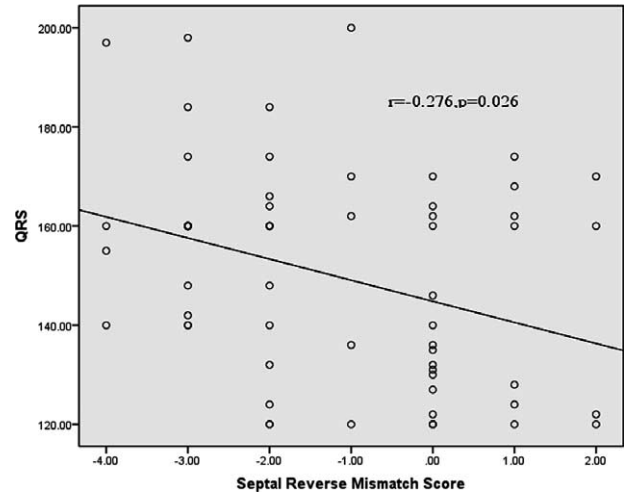

FIGURE 2. Correlation between the QRS interval and the septal reverse mismatch score.

Ono et al. suggested that it is probable that the increased septal IMP (Intramyocardial Pressure) during the T_D(The T_D phase included the major component of LAD flow and was mainly diastolic) phase of the LBBB pattern caused a compression of the septal vessels and increased the coronary vessel resistance, thereby resulting in the reduced myocardial perfusion in the septum, and with impaired thickening during LBBB induced parallel reduction of myocardial glucose uptake in the septum.[22] Impaired septal ^{18}F-FDG uptake that is not paralleled by a concordant reduction of flow to the myocardial septum must be the result of impaired transmembranous transport and/or phosphorylation kinetics.[23]

Clinical Importance

LBBB induces inhomogeneous activation and deformation of the ventricles, leading to inefficient contraction. This regional workload redistribution is associated with important changes in glucose utilization, which is lowest in the septum and highest in the lateral wall region.[2] Higgins et al. suggested that abnormal septal wall motion and impaired wall thickening, in conjunction with perfusion defects, are more likely false-positive findings, whereas normal wall motion and normal wall thickening with septal perfusion abnormalities are indicative of CAD in patients with LBBB.[24]

Limitations

This study was limited by the semi-quantitative, rather than quantitative, nature of the myocardial perfusion and the myocardial metabolism scores. Further, the study was limited by the relatively small number of patients, despite involving 1 of the largest patient populations reported for this type of study.

CONCLUSIONS

In this study, CAD patients with LBBB were found to frequently demonstrate septal and anterior wall reverse mismatches in myocardial perfusion and metabolism, even in the presence of reduced myocardial perfusion. Furthermore, the septal reverse mismatch score was found to negatively correlate with the QRS interval. To further validate the correlation between myocardial perfusion and myocardial metabolism in CAD patients with LBBB, an investigation involving larger groups of similar patients is warranted.

ACKNOWLEDGMENTS

This work was partially supported by grants from the Natural Science Foundation of China (81320108014, 30970849) and the National Science & Technology Pillar Program in the 12th Five-year Plan Period, China (2011BAI11B02).

REFERENCES

1. Jeevanantham VMK, Sengodan M, Haley JM, et al. Predictors of coronary artery disease in patients with left bundle branch block who undergo myocardial perfusion imaging. *Cardiol J.* 2009;16:321–326.
2. Masci PG, Marinelli M, Piacenti M, et al. Myocardial structural, perfusion, and metabolic correlates of left bundle branch block mechanical derangement in patients with dilated cardiomyopathy: a tagged cardiac magnetic resonance and positron emission tomography study. *Circ Cardiovasc Imag.* 2010;3:482–490.
3. Nowak B, Sinha AM, Schaefer WM, et al. Cardiac resynchronization therapy homogenizes myocardial glucose metabolism and perfusion in dilated cardiomyopathy and left bundle branch block. *J Am Coll Cardiol.* 2003;41:1523–1528.
4. Fahy GJPS, Miller DP, McCabe N, et al. Natural history of isolated bundle branch block. *Am J Cardiol.* 1996;77:1185–1190.
5. Hesse BDL, Snader CE, Blackstone EH, et al. Complete bundle branch block as an independent predictor of all-cause mortality: report of 7,073 patients referred for nuclear exercise testing. *Am J Med.* 2001;110:253–259.
6. Lazarus BCE, Thompson PD. Comparison of the results and reproducibility of arm and leg excercise test in men with angina pectoris. *Am J Cardiol.* 1981;47:1075–1079.
7. Pavlovic S, Sobic-Saranovic D, Djordjevic-Dikic A, et al. Comparative utility of gated myocardial perfusion imaging and transthoracic coronary flow reserve for the assessment of coronary artery disease in patients with left bundle branch block. *Nucl Med Commun.* 2010;31:334–340.
8. Altehoefer CvDJ, Buell U. Septal glucose metabolism in patients with coronary artery disease and left bundle-branch block. *Coron Artery Dis.* 1993;4:569–572.
9. Altehoefer CvDJ, Bares R, Stocklin GL, et al. Metabolic Mismatch of septal beta-oxidation and glucose utilization in left bundle branch block assessed with PET. *J Nucl Med.* 1995;36:2056–2059.
10. Zanco PCF, Fini A, Cargnel S, et al. Myocardial perfusion, glucose utilization and oxidative metabolism in a patient with left bundle branch block, prior myocardial infarction and diabetes. *J Nucl Med.* 1998;39:261–263.
11. Civelek ACGIDK, Ozguven MA, Brinker JA, et al. Detection of left anterior descending coronary artery disease in patients with left bundle branch block. *Am J Cardiol.* 1992;70:1565–1570.
12. Lindner O, Vogt J, Baller D, et al. Global and regional myocardial oxygen consumption and blood flow in severe cardiomyopathy with left bundle branch block. *Eur J Heart Failure.* 2005;7:225–230.
13. Neri GZP, Zanon F, Buchberger R. Effect of biventricular pacing on metabolism and perfusion in patients affected by dilated cardiomyopathy and left bundle branch block: evaluation by positron emission tomography. *Europace.* 2003;5:111–115.
14. Nowak B, Stellbrink C, Sinha AM, et al. Effects of cardiac resynchronization therapy on myocardial blood flow measured by oxygen-15 water positron emission tomography in idiopathic-dilated cardiomyopathy and left bundle branch block. *Am J Cardiol.* 2004;93:496–499.
15. Wu YWNM, Tsukamoto T, Komatsu H, et al. Heterogeneous Reduction of Myocardial Oxidative Metabolism in Patients With Ischemic and Dilated Cardiomyopathy Using C-11 Acetate PET. *Circ J.* 2008;72:786–792.
16. Thompson KSG, Birnie D, Chow BJ, et al. Is Septal Glucose Metabolism Altered in Patients with Left Bundle Branch Block and Ischemic Cardiomyopathy? *J Nucl Med.* 2006;47:1763–1768.
17. Candell-Riera JGO-M, Pereztol-Valdés O, Castell-Conesa J, et al. Usefulness of myocardial perfusion SPECT in patients with left bundle branch block and previous myocardial infarction. *Heart.* 2003;89:1039–1042.
18. Zanco PDA, Mobilia G, Cargnel S, et al. Effects of Left Bundle Branch Block on Myocardial FDG PET in Patients Without Significant Coronary Artery Stenoses. *J Nucl Med.* 2000;41:973–977.
19. Wang L, Wei HX, Yang MF, et al. Phase analysis by gated F-18 FDG PET/CT for left ventricular dyssynchrony assessment: a comparison with gated Tc-99m sestamibi SPECT. *Ann Nucl Med.* 2013;27:325–334.
20. Castro P, Winter JL, Verdejo H, et al. Relationship between mechanical and metabolic dyssynchrony with left bundle branch

block: evaluation by 18-fluorodeoxyglucose positron emission tomography in patients with non-ischemic heart failure. *J Heart Lung Transpl.* 2012;31:1096–1101.

21. Hirzel HOSM, Nuesch K, Buettner C, et al. Thallium-201 scintigraphy in complete left bundle branch block. *Am J Cardiol.* 1984;53:764–769.
22. Ono SNR, Kambara H, Okuda K, et al. Regional myocardial perfusion and glucose metabolism in experimental left bundle branch block. *Circulation.* 1992;85:1125–1131.
23. Altehoefer C. LBBB: Challenging Our Concept of Metabolic Heart Imaging With Fluorine-18-FDG and PET? *J Nucl Med.* 1998;39:263–265.
24. Higgins JP, Williams G, Nagel JS, et al. Left bundle-branch block artifact on single photon emission computed tomography with technetium Tc 99m (Tc-99m) agents: mechanisms and a method to decrease false-positive interpretations. *Am Heart J.* 2006;152:619–626.